

Giant-bubble estimation methodology and results

Matthew Roughan

ARC Centre of Excellence for Mathematical & Statistical Frontiers,
the School of Mathematical Sciences at the University of Adelaide,
Adelaide 5005, SA, Australia.

Ph: +618 8313 6282

<http://www.maths.adelaide.edu.au/matthew.roughan/>
matthew.roughan@adelaide.edu.au

SUMMARY

This document provides a detailed description of the mathematical calculations performed to establish the dimensions and volume of the bubbles created on June 19th, in Adelaide, South Australia, by Graeme Denton as part of a World Record attempt to create the world's largest free floating (indoor) soap bubble. The report, based on my expertise as a mathematician, attests that Graeme created, within Guinness World Records guidelines and rules pertaining to the creation, a bubble with volume 19.8 cubic metres or 699 cubic feet.

I. INTRODUCTION

Measuring the enclosed volume of a large soap bubble is a challenging task. Traditional means of measuring volume will not work. For instance:

- We cannot measure a bubble size directly because of its fragility.
- We cannot use the volume of regular solids because giant soap bubbles are not regular.
- We cannot use displacement volume because a soap bubble does not displace, but rather it encloses volume.

The problem is made yet more difficult because soap bubbles are transient – they exist for short periods, and during those periods giant bubbles constantly change shape. Moreover, even modern techniques such as computer vision would find this type of problem challenging because we cannot see the thin film that makes up a soap bubble directly. Rather we actually see specular reflections of external light sources, and these reflections often experience directionally different colour distortions due to the nature of destructive interference at particular wavelengths in the thin film itself. These type of reflections mean that identifying points to key into stereo vision of that bubble is almost impossible (with one notable exception we shall use below).

Instead, in this report, we make use of a mathematical model of the bubbles formation, fitting data to that model in order to provide a computable volume.

The approach makes some simplifying assumptions, however they appear less limiting than those used in the past for bubble volume estimation, and well coupled to the actual formation process. Moreover, in our analysis, we exclude those bubbles that obviously deviate from the model.

In addition, we have ensured that

- 1) the images used have multiple reference scales, such that the underlying measurements are accurate to within a few centimetres;
- 2) that major perspective distortions introduced by the cameras photographing the bubble are corrected; and
- 3) the estimates come with self-diagnostic figures to allow a lay-person to assess the extent to which they fit the true picture.

Thus, as far as we are aware, the results here form the best existing practice for estimating a giant bubble's volume.

We used these techniques to estimate the volumes of several bubbles produced on June 19th, 2017 by Graeme Denton, and show that these consistently reached a volume of almost 20 cubic metres (over 700 cubic feet), more than twice the volume of the current existing record for the world's largest free floating (indoor) soap bubble (8.5 cubic metres).

In particular, at 6:39:24 am, again at 6:40:45, we photographed free-floating bubbles, the best estimates of their volume being 19.9 and 19.8 cubic metres (approximately 700 cubic feet). Detailed dimensions of each are provided in Section IV.

With respect to the Guinness World Records Guidelines for Bubble Records, this document provides a detailed description of the mathematical calculations performed to establish the dimensions and volume of these bubbles. In the following section we provide an elaboration in detail of the proposed procedure submitted prior to the attempt, and how we verified its correctness.

II. METHODOLOGY

A. Setup

The bubble record attempt was held in the gym at Lockley's Primary School, in Adelaide, South Australia. On June 18th, we setup the gym for the attempt that would be conducted the following morning.

The core of the approach adopted here is to photograph the bubble from multiple angles, and use these to estimate the bubble's size.

It is critical for such an estimate that there be accurate measurements present in the photographs, both to estimate the camera parameters (and hence the projection distortions in the images), and to estimate scales for the bubble.

We measured all key lengths in the gym, in particular of the lines marked on the floor within the area of interest. All together, we measured around 20 distances, shown in Figure II.1.

In addition, we placed several large rulers or scales, marked at intervals of 10cm in visually important parts of the field of view: two horizontal a floor level, and a third vertical reference. These provide a secondary distance reference in the images against which to check and confirm any data. We also included six "witches hats" in order to visually highlight key points in the image, so as to avoid missing these through foreshortening of images, or any other distortions of the images.

In addition, in order to ensure that photographs from multiple angles were correctly synchronised, we included a digital clock, displayed by a single computer onto multiple monitors. This ensures that any pair of photographs were synchronised to the nearest second.

A number of other details, not germane to my estimates, were also conducted as part of setup. For instance, a black curtain was hung on the rear wall to provide good contrast so the the bubble was more obvious in photographs, and matting was laid on the floor to absorb moisture released by the bubbles so as to avoid damaging the gym, and provide a safe, non-slip, surface for participants. These preparations were all secondary to the bubble formation, and had no direct impact on measurement or formation. For instance, although the matting covered some of the lines, we ensured it did not hide any of the key reference points.

B. Measurements taken during the attempt

Two primary cameras were used during the bubble attempt. One was placed such that it would have a clear side view of the bubble (and calibration measurements), and the other such that it would have an end view. See Figure II.1 for details of the camera details, and the locations, orientations, and fields of view of the camera*.

*Note that the location, orientation, and field of view of the cameras pictured in the figure are approximations that were estimated more accurately using the camera calibration procedure that follows.

The camera location, and lens setups of the cameras were chosen specifically to be in the mid-range of focal lengths, where non-linear lens distortions (barrel and pin-cushion distortion, for instance) are minimal. Thus we avoid needing to correct for non-linear distortions of this form.

Additional cameras were also used to

- 1) provide video of the attempt;
- 2) provide additional images, should one of the primary cameras fail, and against which we can compare models.

As it happened, the primary cameras functioned flawlessly, and hence the secondary images were not needed for estimation, but are available for verification of the attempt as needed.

Figure II.4 shows an example of a pair of images from the primary cameras taken at 6:40:45 am (all figures displayed will be based on the images acquired at this time point).

C. Estimation Methodology

1) *Camera calibration:* It is almost inevitable that during a set of photographs, even a tripod mounted camera may be moved slightly. Small movements of location are relatively trivial, however, small changes in the orientation, of less than 1 degree of arc can change the field of view of the camera significantly. And small changes in the focal length settings of lens can also have a significant effect.

It is therefore important that each image of the bubble attempts was individually calibrated.

This calibration was performed by identifying 10 reference points in the gym, whose location was established to the nearest cm by physical measurement using a standard measuring tape (see above). The particular locations chosen were corners of the witches hats (where the lines intersected), the intersection of the red line with the yellow and white lines, and the bottom and top marked lines of the vertical scale. The points were chosen to be visually identifiable in both primary camera images. Figure III.1 shows a schematic of the reference points used.

Any 4 of these should be sufficient to calibrate an image, the additional points were included to check any errors in calibration. The reference points were manually selected from each image to provide accurate locations. It should be noted that although reference points were originally measured down to the nearest cm, the foreshortening of the photographs may have magnified this error in some images to as much as 3-5cm.

Camera data was also obtained from the EXIF data present in the image. The specific information needed here was the current focal length of the lens when the photograph was taken. Exposure speed and other related details were also retained, though they have little effect on the results, except that we note that all exposures were for less than 1/50th of a second, allowing a precise capture of the bubble despite its motions.

The calibration was performed using software written for the purpose in Matlab. It was implemented using a non-linear optimisation routine to find the best set of camera

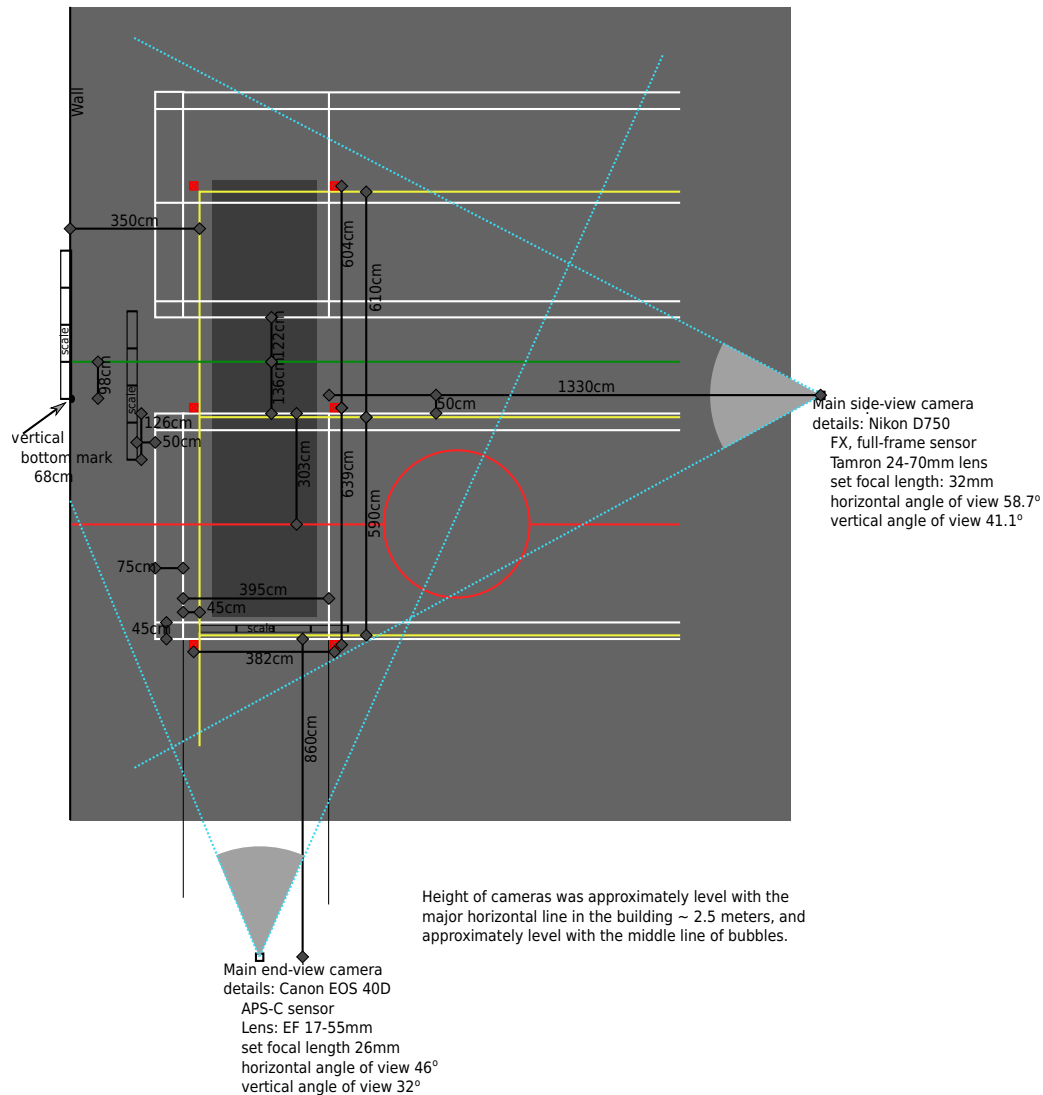


Fig. II.1: The gym schematic with measurements, locations, orientations and fields of view of the primary cameras, and locations of additional scales and witches hats. The figure is approximately to scale. All measurements were to centres of lines, and to the nearest cm.

parameters (location, and orientation) to explain the reference point locations in each image. Once we have obtained the camera parameters accurately, these are used in subsequent computations.

D. Perspective correction and the location of the bubble

As noted above, we chose camera position, and lens setup so as to minimise barrel and pin-cushion distortions, but any photographic image will contain perspective distortions.

Perspective distortion (in images) refers to the fact that objects further from the viewer (be they camera, painter, or any other observer), appear smaller [1].

Correcting perspective distortion is therefore critical in estimating true dimensional measurements in an image.

Perspective distortions are described by a set of mathematical relations described in [1]. The important parameters in these distortions were estimated in our camera calibration procedure, and hence we can calculate the effect of these distortions precisely. Figure II.2 illustrates the estimate projection distortion for the side-view image.

There exist software to correct for perspective distortion, however we wrote specific software to correct it in Matlab, in order that we have a consistent tool-chain, built in the same software, to perform the entire bubble measurement task.

The software uses two images, and the relevant camera calibration data for those cameras, to take a point designated in two images, and derive its location in 3-dimensional space.

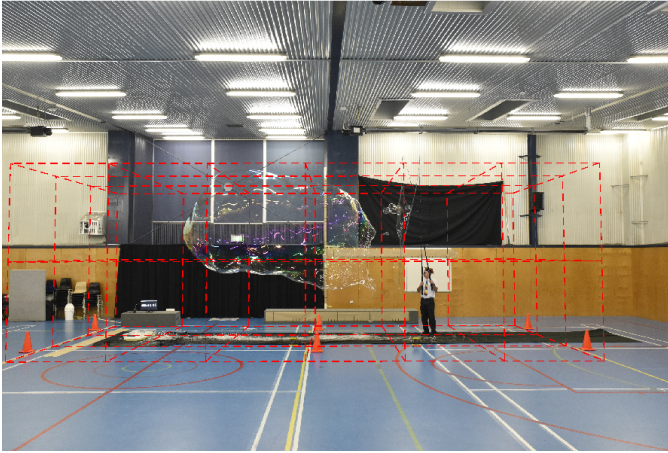


Fig. II.2: Projected grid to illustrate the effect of projection distortion on the image. The grid cubes have 2m sides.

As noted earlier, it is difficult, if not impossible to determine the same point in two images of a bubble. In most cases we cannot see the *bubble* itself, but rather we only see reflections from light sources, and as these differ dramatically from the two cameras' viewpoints, we cannot find common points.

However, in addition to reflections, we can also see the “edge” of the bubble. When examined in profile, the edge forms a much thicker cross-section than the typical thin-film of the bubble’s surface. This thicker cross-section results in diffraction, which makes the edge visible, even in the absence of reflections. See, for instance, Figure II.3.

Thus there is at least one identifiable point on all such bubbles, its *peak*. That is, the topmost point on the bubble will be visible, and identifiable in both primary camera views. We perform this identification manually, to ensure accuracy, and then the the software described above to estimate its position in 3-dimensional space, thus providing a point of reference for all further measurements.

E. Modelling

As noted earlier, apart from the point described above it is difficult to reliably find other points on a bubble that can be identified from multiple points of view. It might be thought that others (such as the lowest point) would also be suitable, but unfortunately the lower part of the bubble is usually more irregular, and so multiple points may sometimes be confused. Hence, we must relate other points in the images to the one reliable reference point.

We do so by introducing a mathematical model for the bubble, based on its formation procedure.

The nature and behaviour of bubbles has been known for many years, *e.g.*, see [2]. The fact most well known is that soap films act under surface tension to minimise their surface area, and therefore a bubble enclosing a fixed volume will tend towards a sphere, which is the mathematical shape that has minimal surface area for a given volume.

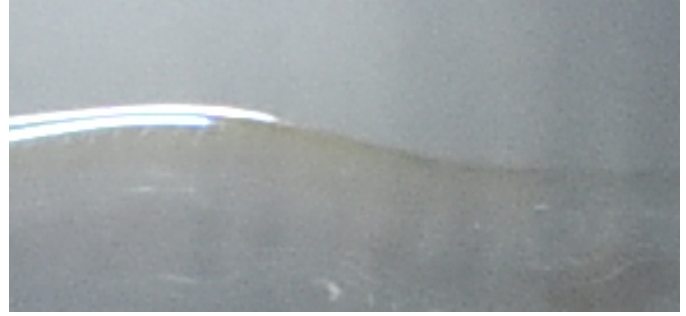


Fig. II.3: View of the edge of a bubble. Note that the edge of the bubble is visible even in absence of a strong reflection.

However, surface tension is proportional to the shape’s curvature, and hence for very large bubbles, such as considered here, the surface tension forces are small compared to the forces acting on the bubble (gravity and random motions of the air around the bubble), and hence large soap bubbles are rarely spherical. In fact, they largely retain the shape in which they are formed. However, surface tension does tend to lead to somewhat smoothed shapes.

The formation process for large bubbles involved (in this case specifically, but also in many other attempts), using two long wands holding a loop of soap-impregnated cord that are passed through a volume of space. As they do so, the soap film formed inside the loop is stretched by the air, and forms a long “tube” of soap film. The tube is eventually closed off by bringing the wands together and closing the loop.

Thus, in many cases, the resulting bubble is shaped like a sausage, whose cross-sections are determined by the shape of the loop as it passes through the air. A first model might approximate the loop as circular, or oval, but as it happens, the particular details of the setup: the lift, the orientation of the bubble’s creator, and the exact environment at the time of formation cause changes in the shape of this cross-section. Thus we might think of these bubbles as slightly irregular sausages, and it is this we will model.

We approximate the bubble shape by the surface given by the equations

$$y(x, \theta) = r(x) \times c_y(\theta), \quad (\text{II.1})$$

$$z(x, \theta) = r(x) \times c_z(\theta). \quad (\text{II.2})$$

where x is the direction of motion of bubble formation (along the length of the sausage), $r(x)$ is the generalised radius of the sausage at any point x (we will call these *longitudinal radii*), and the $c_i(\theta)$ describe the curve that gives shape of the cross-section in terms of the angle θ , from 0 to 360 degrees, representing a rotation around the x -axis. See Figure III.2 for an illustration of this shape for a real bubble.

Thus, in order to estimate this shape accurately, we need to estimate $r(x)$ and $c_i(\theta)$. We do so from the primary images. In each, we selected a detailed set of points along the edge of the bubble, shown in Figure II.4.



Fig. II.4: Bubble edge selections shown as red lines. Note that the protuberance at the bottom of the end-view image, and the final irregular component of the bubble caused by closure are omitted, thus the model encloses a region smaller than the actual bubble.

There is no doubt that this approximation is just that. It is not the exact shape of the bubble, just a best estimate of it. In order to minimise the chance that we overestimate the bubbles volume, we estimate the cross-section and longitudinal radii conservatively, omitting any protuberances. Thus the volumes calculated here are *lower-bounds*, *i.e.*, the real volume of the bubble should exceed our somewhat conservative estimate. In addition, we originally selected a larger number of bubbles for analysis, but did not include any that showed any marked deviation from this model, to avoid large modelling errors.

The reference curves around the edge of the bubble will be given in image coordinates. We can directly estimate the c_i from this, as we need only relative shape, but we cannot directly estimate $r(x)$ because this needs to be given in real (not image) units.

We use our point of reference at the peak of the bubble to convert obtain $r(x)$. We first place the side-view of the bubble into 3D spatial coordinates by assuming that the bubble is oriented along the spatial x -axis. We further make the initial assumption that the axial cross-section is symmetric, to estimate the location of the centre-line of the bubble. However, the bubbles are not axially symmetric, as can be seen in Figure II.4, and so this is only used as an initial value.

Given the centre-line of the bubble and the symmetry assumption, we can correct the perspective distortions of the entire the edge on view of the bubble, to obtain its longitudinal radius in real units. From this we can estimate the entire surface. Once we have an initial estimate of the surface, we can correct the error induced by the symmetry assumption, to obtain the true center-line, and from there we repeat the procedure above to estimate the model surface.

F. Volume calculation

The volume is calculated by numerical integration of the surface given above. The procedure is simplified dramatically by the model, which allows us to integrate the z and y terms separately, obtaining a normalised cross-sectional area, which we then numerically integrate (a procedure sometimes called *quadrature*) in the x -direction using 10,000 points on the grid. Alternative numbers of points on the grid were trialled, 10,000 points having errors much less than 1%, *i.e.*, negligible compared to other sources of error.

The modelling was performed with additional software written in Matlab, as was the volume estimation software.

III. VERIFICATION METHODOLOGY

An important aspect of any measurement is calibration of the measurements, however, the inherent reason for this methodology is that we have no “calibration bubble” with a precisely known volume, against which we can test. Even if we could conceivably have such, we would need many in order to understand the effect of variations in shape and location on the measurement methodology, and this is entirely impractical.

Instead, we can validate each step in the process, thus allowing a measure of confidence in the overall result. This section documents the tests performed to validate each step above. Some are formal, quantitative tests. Others are more qualitative, but never-the-less useful to obtain a complete understanding of the estimation accuracy.

The first test is to check images for non-linear barrel and pin-cusion type distortions. These would cause (non-radial) straight lines in the images to appear curved. As we can see from Figure II.4, the straight lines in the images appear straight, with the possible exception of minor distortions towards the edge of the image, well away from the region

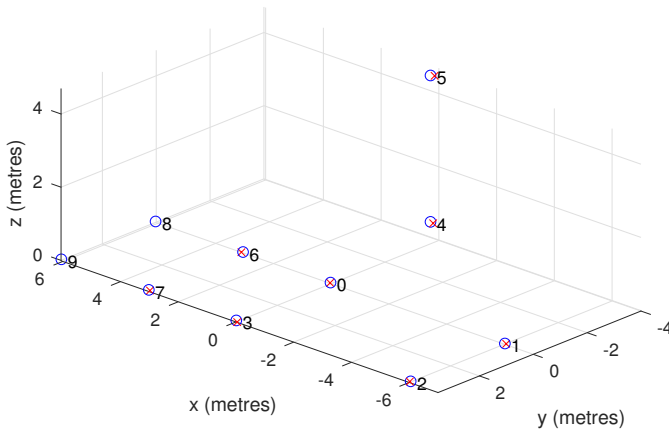


Fig. III.1: Reference markers (blue o), and their estimated position via inverting the perspective distortions of a pair of images (red x). Points 0-4, and 8,9 refer to corners of witches hats, 4 and 5 to the vertical upright, and 6 and 7 to intersections of the red line with the yellow and white lines, respectively.

of the bubble. Hence we believe such distortions to have negligible effect here.

The next test is to consider how well our perspective transformation works. There are errors in the marking of our reference points of the order of 4-5 cm due to image resolution and foreshortening, and these may feed into errors in the camera parameters, which may then feed into our perspective distortion estimates, and we aim to estimate these here.

We are able to perform this test because we selected a larger number of reference points than are needed. Thus, we can invert the perspective transform on these points based on a pair of images, and compute the errors between their estimated position and their true position. Figure III.1 shows the origin reference points (blue o), compared to the points obtained by correcting perspective from a pair of images (red x). One can visually see that the points correspond, but more important are the quantitative differences. The largest positional error along the y -axis (the axis most crucial for our volume estimation), is 4.4 cm. That is, the errors in the perspective transformation are of the order of the errors in reference point selection in the images. We will consequently assume in what follows an error bound of ± 5 cm.

The second major form of validation is to compare the model bubble with the true bubble. As a matter of construction, the bubble will seem similar from the viewpoints of the two primary cameras. However, using Matlab, we can construct a 3D surface. The surface can then be rotated and examined from various angles, comparing it to other images, to ensure that the bubble is a realistic model of the true bubble. Figure III.2 shows the bubble surface from one such angle, and modulo the smoothing effect of removing protuberances, we can see

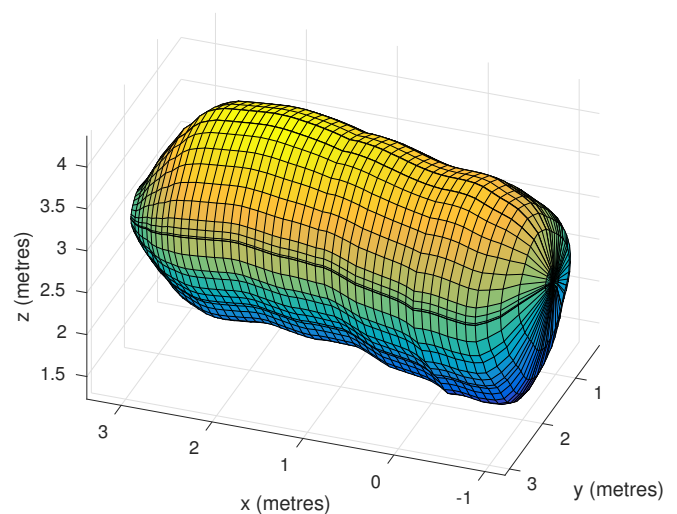


Fig. III.2: Model bubble.

that it reasonably approximates the true bubble.

We then use the errors in the y -axis estimates to estimate the errors in volume estimation. The reference point obtained at the peak of the bubble is shifted by the maximum perspective induced errors, and the volume recalculated. This provides our upper and lower bounds on volume estimates that vary from the estimate by $\pm 0.1m^3$, *i.e.*, one tenth of a cubic metre.

The modelling errors, arising from the simplifying assumptions of the model could be larger than this, but we have ensured by selecting only bubbles that fit the model well, and by eliminating protuberances, that the modelling errors are positive, *i.e.*, the model provides a conservative lower bound on the true volume, so we do not attempt to report these errors. However, it should be noted that the true volume might be as much as 10% more than the volume calculated here.

IV. RESULTS

The bubble creation attempt took place between approximately 6 and 7am, June 20th, 2017. Over this period, several dozen bubbles were created.

It was determined after the attempt (from photographs and videos) that at least six large bubbles satisfied the Specific Guidelines for Bubble Records, in particular for the largest free-floating soap bubble. They were free floating, closed, soap films with large proportions.

These six were considered further in case our stringent guidelines for inclusion were not met.

We conducted the above procedure on each. Two bubbles were omitted from consideration because they deviated significantly from the model. Two more are omitted here because they were somewhat smaller. The results here are listed in Table I for the two largest, that satisfied all criteria.

Dimension	Bubble	
	6:39:24	6:40:45
Max. height (m)	2.7	2.7
Max. width (m)	2.4	2.9
Max. length (m)	6.1	4.6
Total volume (m^3)	19.9	19.8
Total volume (ft^3)	702	699

TABLE I: Bubble dimensions. Height refers to how tall the bubble is, not how high above the ground it is. That is, height is the extent of the bubble along the z -axis as pictured. Length and width are the maximum extent along the x and y axes, respectively. The two bubbles are denoted by the time at which the relevant pictures were taken. Volume estimates are $\pm 0.1m^3$.

We list two bubbles to show the consistency of the estimation methodology, *i.e.*, bubble volumes were consistent, despite somewhat different shapes.

The most important result is that the bubble volumes were 19.9 and 19.8 cubic metres in volume, with an error induced by perspective of ± 0.1 cubic metres. The most elegant, and long-lived of the pair was the second, and so it is this we submit for the record (despite the fact it is slightly smaller). All included images in this report relate to this particular bubble.

V. CONCLUDING MATERIALS

This report documents my (Prof Matthew Roughan's) measurements and calculations of the world's largest free floating soap bubble (indoors).

In particular, with respect to the Specific Guidelines for Bubble Records, this document provides a detailed description of the mathematical calculations performed to establish the dimensions and volume of said bubble.

A. Expertise

My expertise in this field arises from a PhD in Applied Mathematics, as well as an Honours Degree (1st class) in Physics, and Bachelor of Science degree with a triple major in Mathematics, Physics and Computer Science. I have more than 20 years of experience since completing my degree, much of it in modelling and interpreting measurements. Additionally,

I have taught advanced (3rd year) mathematical classes at the University of Adelaide (where I am currently employed) including material on the mathematics of soap films.

B. Compliance

I declare that I am not associated with, or related to Graeme Denton, nor have anything to gain from the final outcome of the attempt.

I observed the setup of the gym on June 18th, and the bubble creation attempts on June 19th (2017).

As far as I am aware, Graeme Denton and all other persons involved in the attempt complied with all Guinness World Records guidelines in making the attempt, including the general guidelines, and the guidelines specific to this record.

In fact, in my expert opinion, Graeme exceeded all requirements, in order to ensure that the results be beyond reproach, and I would suggest that in future attempts, additions be made to the guidelines to ensure that future attempts are as accurately measured.

REFERENCES

- [1] I. Carlbom and J. Paciorek, "Planar geometric projections and viewing transformations," *ACM Computing Surveys*, vol. 10, no. 4, pp. 465–502, 1978, <http://www.cs.uns.edu.ar/cg/classes/pdf/p465carlbom.pdf>.
- [2] C. Isenberg, *The Science of Soap Films and Soap Bubbles*. Courier Dover, 1978.

Name



Signature

28th June, 2017

Date